Tetragonal magnetic phase in $Ba_{1-x}K_{x}Fe_{2}As_{2}$ from x-ray and neutron diffraction

J. M. Allred, S. Avci, D. Y. Chung, H. Claus, D. D. Khalyavin, P. Manuel, K. M. Taddei, M. G. Kanatzidis, S. Rosenkranz, R. Osborn, and O. Chmaissem

Phys. Rev. B **92**, 094515 — Published 28 September 2015

DOI: 10.1103/PhysRevB.92.094515

Tetragonal magnetic phase in $Ba_{1-x}K_xFe_2As_2$ from x-ray and neutron diffraction

J. M. Allred,[1,*] S. Avci,[1,2] D. Y. Chung,[1] H. Claus,[1] D. D. Khalyavin,[3] P. Manuel,[3] K. M. Taddei,[1,4] M. G. Kanatzidis,[1,5] S. Rosenkranz,[1] R. Osborn,[1] and O. Chmaissem[1,4]

[1]*Materials Science Division, Argonne National Laboratory, Argonne, IL 60439-4845, USA*
[2]*Department of Materials Science and Engineering, Afyon Kocatepe University, 03200 Afyon, Turkey*
[3]*ISIS Pulsed Neutron and Muon Source, Rutherford Appleton Laboratory, Chilton, Didcot OX11 0QX, United Kingdom*
[4]*Physics Department, Northern Illinois University, DeKalb, IL 60115, USA*
[5]*Department of Chemistry, Northwestern University, Evanston, IL 60208-3113, USA*

Combined neutron and x-ray diffraction experiments demonstrate the formation of a low-temperature minority magnetic tetragonal phase in $Ba_{0.76}K_{0.24}Fe_2As_2$ in addition to the majority magnetic, orthorhombic phase. The coincident enhancement in the magnetic ($\frac{1}{2}$ $\frac{1}{2}$ 1) peaks shows that this minority phase is of the same type that was observed in $Ba_{1-x}Na_xFe_2As_2$ ($0.24 \leq x \leq 0.28$), in which the magnetic moments reorient along the c-axis. This is evidence that the tetragonal magnetic phase is a universal feature of the hole-doped iron-based superconductors. The observations suggest that in this regime the energy levels of the C_2 and C_4 symmetric magnetic phases are very close.

PACS numbers: 74.70.Xa, 74.25.Ha

I. INTRODUCTION

A key to understanding the pairing mechanism in the superconducting state of the iron pnictide and chalcogenide superconductors is characterizing the nature of the electronic interactions that are responsible for the spin-density-wave (SDW) state that competes with the superconductivity. The origin of the magnetic order, which is coupled to an orthorhombic distortion of the high-temperature tetragonal lattice that is often labelled 'nematic' order, is still debated, with a range of theoretical treatments that range from localized orbital models to weak-coupling itinerant models based on Fermi surface nesting.[1–3]

Since it seems that, until now, each class of models could be modified to comport with the measured properties, solely studying the principal SDW state is apparently not enough to settle the dispute. Recently we have shown that a second tetragonal magnetic phase appears near the end of the SDW dome in hole-doped $Ba_{1-x}Na_xFe_2As_2$ which we called the "C_4" phase to distinguish it from the more usual stripe SDW phase, which has "C_2" symmetry.[4–6] The magnetic component of the C_4 phase transition was shown to come from the reorientation of the moments from in-plane to out-of-plane.[7,8] The reorientation temperature, T_r, occurs well above T_c, indicating that it does not arise from a coupling of the superconducting order parameter with the other order parameters as was observed in $Ba(Fe_{1-x}Co_x)_2As_2$,[9] but instead must be a manifestation of changes in the coupling between iron atoms. Usually symmetry is reduced at low temperature for thermodynamic reasons, so the return to tetragonal symmetry accompanying the magnetic reorientation puts new constraints on the set of plausible electronic ordering mechanisms. A group theory analysis shows that it may be possible to distinguish between itinerant and quasi-local orbital models through the observation of orbital order in the C_4 phase.[8]

As such, it is important to establish whether this phase is unique to the $Ba_{1-x}Na_xFe_2As_2$ system, or whether it is observed in other related systems, in order to decide if the inferred physics of these specific compounds are atypical or more general. Related families such as the hole-doped $Ba_{1-x}K_xFe_2As_2$ have been extensively studied in earlier publications.[10,11] Here we return our attention to the region near the edge of the dome of $Ba_{1-x}K_xFe_2As_2$ using fine temperature control with both high-resolution x-rays and high-intensity neutrons. The combined analysis shows that the reentrant C_4 tetragonal phase is indeed present in the $Ba_{1-x}K_xFe_2As_2$ phase diagram at $x = 0.24$, but not below $x = 0.22$, indicating that it is a common feature of the hole-doped '122' iron compounds. It is only present as a minority phase below a first-order transition, consistent with the delicate energy balance between the C_2 and C_4 phases predicted by itinerant spin-nematic theory,[2] and is rapidly suppressed below the superconducting transition. We had earlier reported that the C_4 phase in $Ba_{1-x}Na_xFe_2As_2$ exhibited a stronger competition with superconductivity than the C_2 phase,[4] but this is the first time we have observed the complete suppression of the C_4 phase below T_c.

II. TECHNIQUES

The polycrystalline samples reported in Ref 11 were used in the new measurements. The $Ba_{1-x}K_xFe_2As_2$ samples reported here were previously determined to have the following compositions: $x = 0.225$, 0.237, and 0.249. For simplicity they will be referred to as $x = 0.225$, 0.24, and 0.25, respectively. Powders were prepared by combining stoichiometric amounts of BaAs, KAs, and Fe_2As in sealed Nb tubes, which were in turn sealed in quartz tubes and fired at 1050 ℃. More details

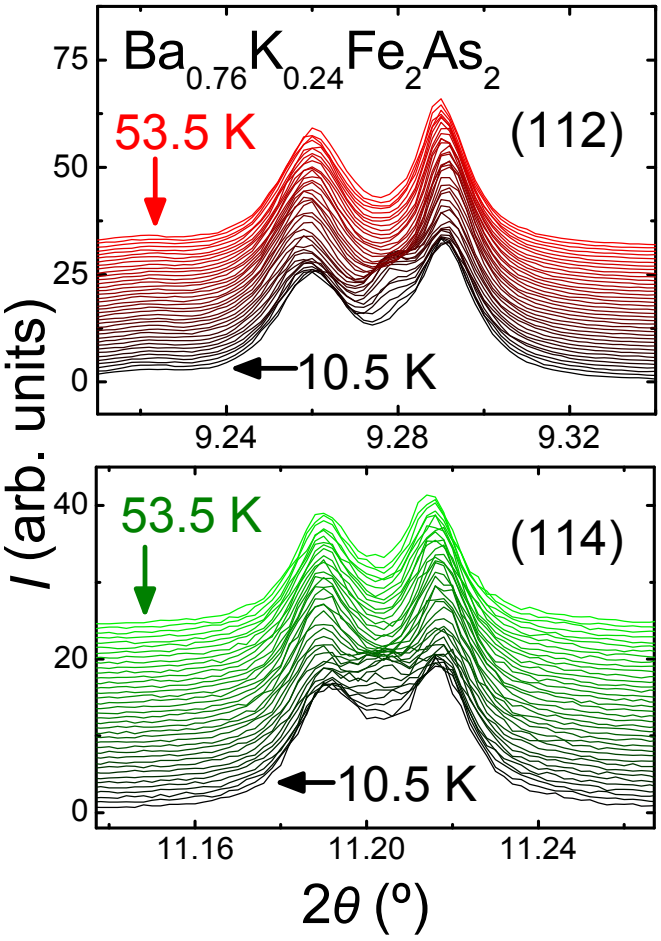

FIG. 1. Overlaid x-ray diffraction scans of $Ba_{0.76}K_{0.24}Fe_2As_2$ at approximately uniform increments from 10.5 to 53.5 K. The top panel shows the (112) reflection and the bottom shows the (114) reflection. The split peak in the orthorhombic phase corresponds to the $(11l)$ and $(\bar{1}1l)$ components (I-cell), which are the $(20l)$ and $(02l)$ peaks in the conventional F-centered cell.

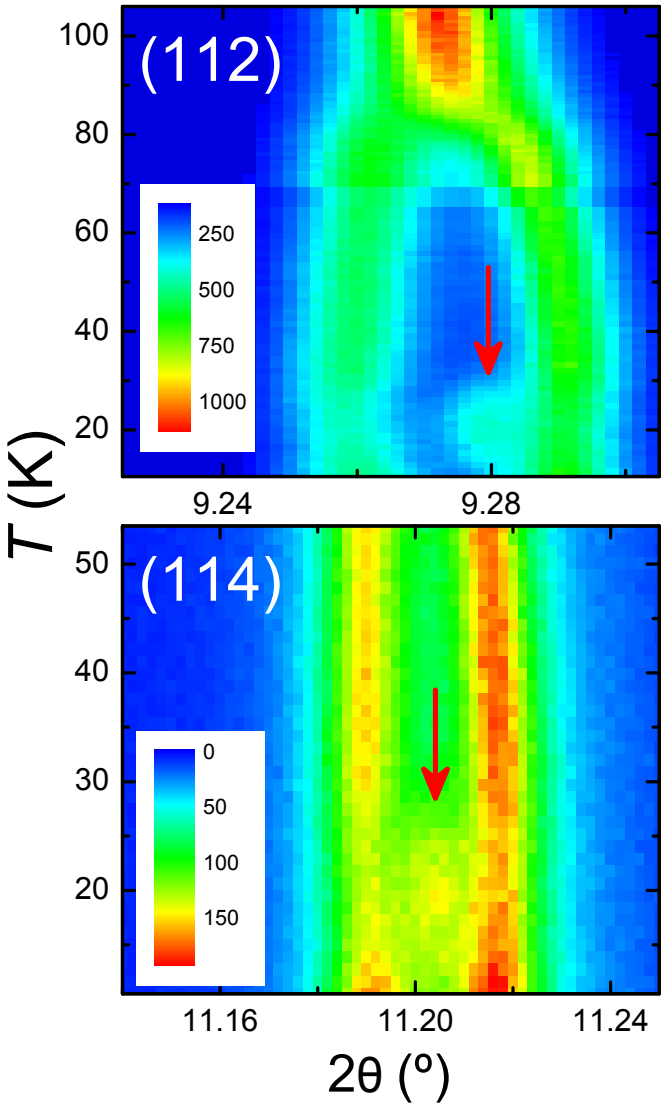

FIG. 2. False color map drawn using the x-ray diffraction data on $Ba_{0.76}K_{0.24}Fe_2As_2$. The top panel shows the temperature range from 10 to 120 K of the (112) reflection, which splits into the (202) and (022) orthorhombic peaks. The bottom panel shows the (114) (corresponding to the (204) and (024) components of the orthorhombic cell) from 10 to 53 K. The arrows point to the peak corresponding to the minority tetragonal phase.

can be found in the original publication.[11] Powder x-ray diffraction experiments (PXRD) were measured at the Advanced Photon Source, Argonne National Laboratory, on beamline 11-BM-B using the liquid helium cryostat ($\lambda = 0.413429$ Å). The sample was prepared for measurement by dusting the outside of a greased kapton capillary with sample powder. 2θ scans were collected approximately every 1 K as the temperature was constantly ramped from ∼10 to 105 K. Rietveld refinements were performed using General Structure Analysis System (GSAS)[12] and the graphical user interface, EXPGUI.[13] Powder neutron diffraction (PND) experiments were performed at ISIS, Rutherford Appleton Laboratory, on the Wish beamline.

III. RESULTS AND DISCUSSION

A. $Ba_{0.76}K_{0.24}Fe_2As_2$

The diffraction data on $Ba_{0.76}K_{0.24}Fe_2As_2$ are summarized in Figures 1, 2 and 3. The peak indices are given for the body-centered tetragonal cell in all cases. The cascaded diffractograms of the x-ray diffraction data (Figure 1) shows the splitting of the (112) and (114) reflections, with clear evidence of a minority phase growing in and disappearing again on warming from 10 ($T_{r,1}$ to 30 K ($T_{r,2}$) between these two reflections. The same data can

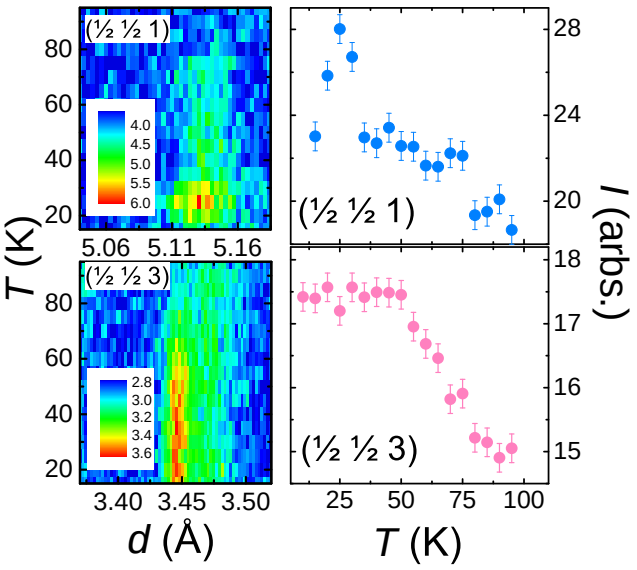

FIG. 3. Left panels: Temperature-dependent color maps depicting the magnetic peak intensity of the $(\frac{1}{2}\ \frac{1}{2}\ 1)$ (top) and $(\frac{1}{2}\ \frac{1}{2}\ 3)$ (bottom) reflections. The right panels are peak intensities integrated from a 5-point-wide cut through the peak of interest.

also be visualized using a false color map, as depicted in Figure 2. The neutron diffraction data (Figure 3) shows an evolution in the magnetic intensity within the same 10 to 30 K region for the $(\frac{1}{2}\frac{1}{2}1)$ reflection. Little change is observed in the $(\frac{1}{2}\frac{1}{2}3)$ peak below 50 K. Previous results from $Ba_{1-x}Na_xFe_2As_2$ showed that the C_4 phase exhibits a 10-fold increase in intensity of the $(\frac{1}{2}\frac{1}{2}1)$ magnetic peak, and a slight reduction in the $(\frac{1}{2}\frac{1}{2}3)$ magnetic peak, resulting from the spin reorientation. Here the magnitude change in the $(\frac{1}{2}\frac{1}{2}1)$ is consistent with an approximately 10% C_4 phase fraction.

A two-phase Rietveld refinement was used to model the minority phase in the 11BM data. For two-overlapping phases of such similar structure, it is difficult to refine the lattice parameters for the minority phase reliably, and similar R values are obtained regardless of whether certain parameters of the tetragonal phase are constrained or allowed to refine freely. For example, freely refining the lattice parameters of the minority phase gives obviously incorrect peak positions, due to convolution with small features in the majority phase peak's shoulders that are not perfectly modeled using conventional Rietveld peak shapes. These values also covary with the relative phase fraction, making a unique solution unattainable. As detailed below, several assumptions and approximations must be made in order to minimize systematic errors and to produce a model that is physically meaningful.

To start, the c-axes of both phases (c_1 and c_2, for the majority orthorhombic and minority tetragonal phases, respectively) were constrained to be equivalent, since no extra broadening of the $(00l)$ reflections was observed when comparing the two-phase and one-phase temperature regions. The shoulders in the peaks split by the orthorhombic distortion (such as what is shown in Figure 1) can then be used to define the other cell axis of the minority phase, a_2, which allows the free refinements of a_1 and b_1, giving good agreement with the data. Thermal and peak profile parameters of both phases were constrained to be equivalent—excepting small differences in the peak profile arising from the differing phase symmetries—which allowed the weight fractions to be refined self-consistently. Using this method, the final two-phase refinement models have all of the crystallographic parameters of the orthorhombic phase freely refined, while, for the tetragonal phase, only the scale factor is refined by GSAS.

The temperature dependence of the lattice parameters of the majority phase is summarized in Figure 4. Note that the missing data around 60 K is due to a limited malfunction of the temperature controller that made quantitative analysis impossible in this temperature range. The refined lattice parameters of the majority (orthorhombic) phase do not appear to be affected by the presence of the minority (tetragonal) phase. For example, the orthorhombic order parameter shows the usual discontinuity at T_c (26 K), but there is no evidence of a change in slope corresponding to the (dis)appearance of the tetragonal phase. This is further evidence that the transition from orthorhombic C_2 phase to the magnetic C_4 phase is of first order and that the two phases are microscopically decoupled. The structural transition at T_s is also clearly in the primitive basal plane lattice parameter (here, called a_{tet}) and orthorhombic order parameter, $\delta = \frac{a_1-b_1}{a_1+b_1}$ (Figure 4 (a) and (b), respectively). Note that δ implies an orthorhombic model was used, even if the sample was concluded to be tetragonal on average. The in-plane lattice parameter, a_{tet}, is calculated from the orthorhombic phase by transforming the conventional F-centered cell back to the I-centered one, *via* $a_{1,tet} = \sqrt{(a_1^2 + b_1^2)/2}$. Below T_N, this value is clearly enhanced, as is typical of hole-doped 122 iron-pnictides,[14] while the c-axis shows little change. The volume anomaly at T_N is primarily seen as a subtle change in slope.

The properties of the minority phase are also plotted in Figure 4(c) and (d). What is observed is a small tetragonal phase fraction that reaches a maximum ($\sim 8\%$) between 20.8 and 22.7 K, and becomes indistinguishable from background below 12 K and above 30 K. The in-plane lattice parameter appears to be rather smaller than the primary phase (Figure 4 (c)). The phase fraction derived from the x-ray data peaks at the same temperature as the enhancement in the magnetic peak intensity of the $(\frac{1}{2}\ \frac{1}{2}\ 1)$ reflection in neutron data. This agrees well with the interpretation that this minority phase is the same tetragonal magnetic phase that was observed in $Ba_{1-x}Na_xFe_2As_2$.[4]. The decrease, and eventual complete suppression, of the C_4 phase fraction below T_c, shown in the inset to Fig. 4d, is consistent with our earlier observation that it competes more strongly with

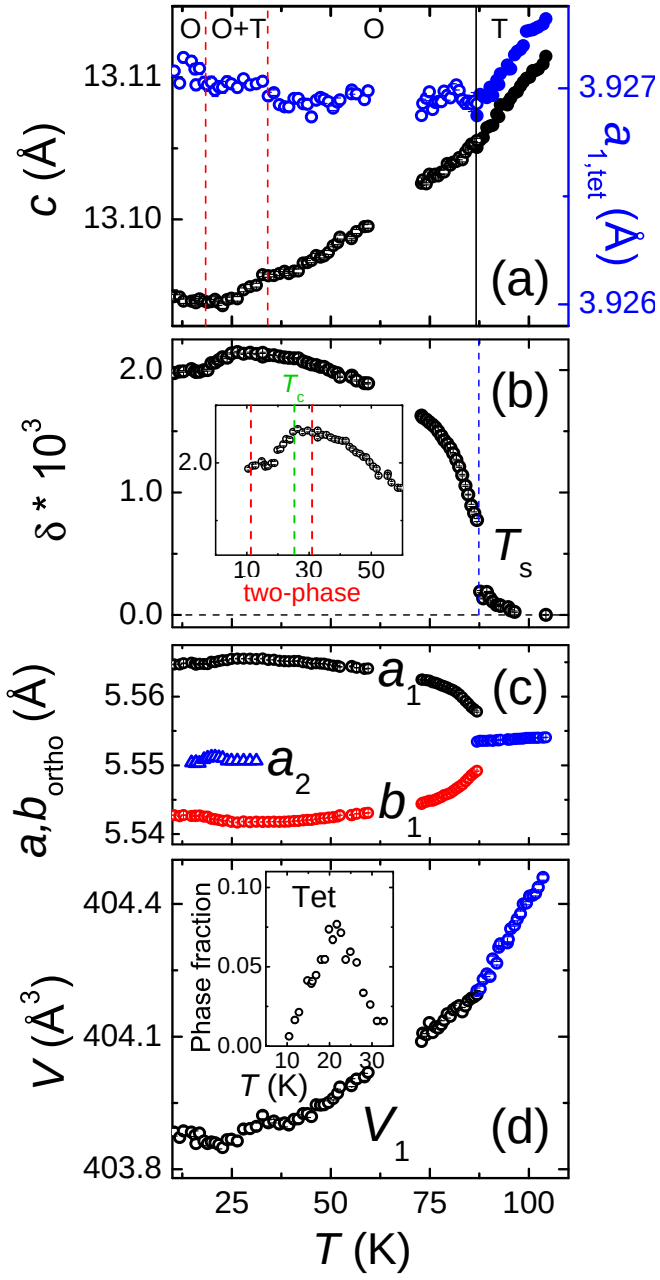

FIG. 4. Refined lattice parameters for the majority phase in $Ba_{0.76}K_{0.24}Fe_2As_2$ determined from x-ray powder diffraction. (a) c_1 is shown in black, and $a_{1,tet}$ in blue (see text). Orthorhombic (open circles) and tetragonal (closed circles) fits were used below and above 87 K, respectively. (b) The major phase orthorhombic order parameter. Inset is a detailed view around T_c and T_r. (c) In-plane lattice parameters (a (black circles) and b (red circles), orthorhombic phase; a_1 (blue circle) and a_2 (blue triangles), tetragonal phases. Tetragonal lattice parameters are scaled by $\sqrt{2}$. (d) The volume of the majority phase (V_1), with blue and black circles being used to demarcate the transition from tetragonal to orthorhombic models, respectively. The inset is the refined phase fraction of the minority phase.

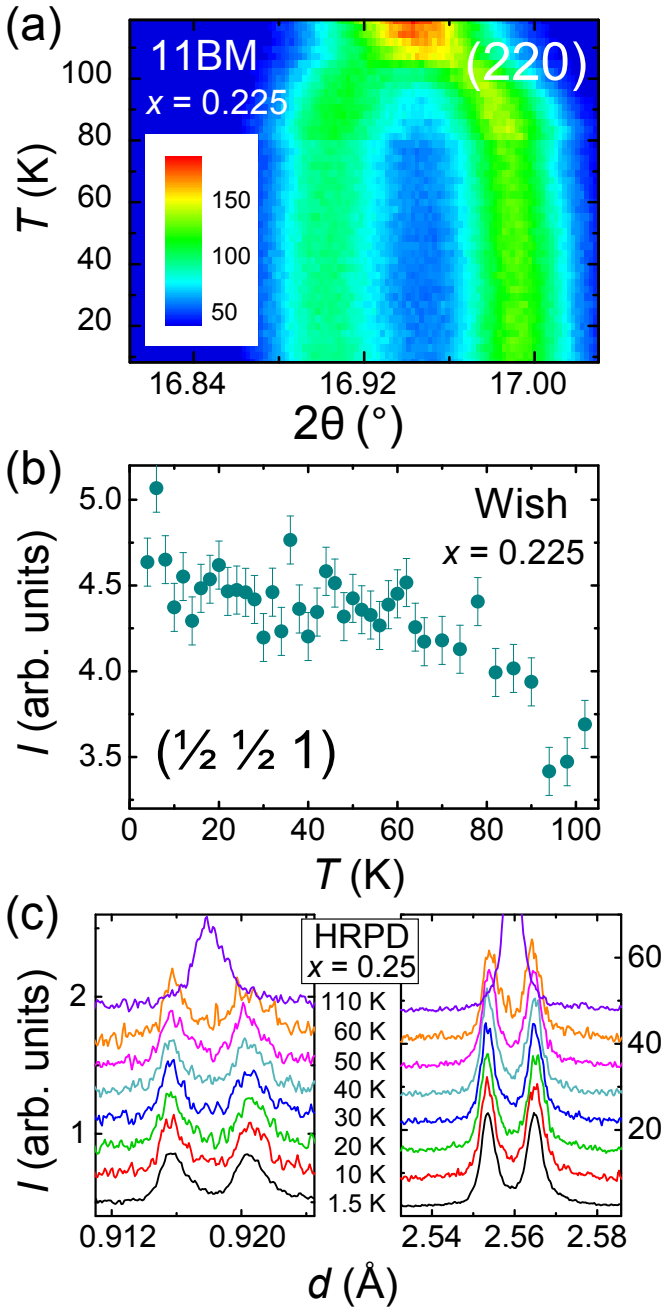

FIG. 5. X-ray powder diffraction data from $Ba_{0.775}K_{0.225}Fe_2As_2$. (a) X-ray (11BM) diffractogram of the (220) reflection. (b) Integrated intensity across the $(\frac{1}{2}\frac{1}{2}1)$ reflection from the neutron (Wish) powder diffraction data. (c) Neutron powder diffraction data (HRPD) on $Ba_{0.75}K_{0.25}Fe_2As_2$ reproduced from Ref. 11

superconductivity than the C_2 phase.[4]

B. $Ba_{0.775}K_{0.225}Fe_2As_2$ and $Ba_{0.75}K_{0.25}Fe_2As_2$

While the above results unambiguously show that the C_4 phase also forms in the K-substituted $BaFe_2As_2$ phase

diagram, it is useful to discuss the scope of this C_4 regime. We performed similar high-resolution x-ray and high-intensity neutron diffraction experiments on a $x = 0.225(10)$ sample, with a temperature spacing of 2 K, which showed no evidence of a lt- (low temperature) tetragonal phase nor of any spin reorientation (Figure 5a and b, respectively). This sets a reasonable lower limit at this composition, since the x-ray and neutron experiments have detection limits of $\sim 1\%$ and 3% phase fractions, respectively.

For a slightly higher composition, $x = 0.25$, no evidence was observed in our previous high-resolution neutron diffraction (HRPD) of a lt-tetragonal phase.[11] The raw data from 1.5 to 60 K are displayed in Figure 5(c) for comparison. With temperature steps every 10 K, the sample appeared entirely single phase orthorhombic below T_N. The detection threshold is slightly higher for HRPD than 11BM, but even a 5% phase fraction would be visible above the noise. Thus, while it is not impossible that the C_4 phase exists in this sample, the temperature window and/or phase fraction must be much smaller than in $x = 0.24$.

C. Extent in Phase Space

Recent uniaxial dilatometry measurements provide evidence of a return to tetragonal symmetry in a narrow temperature range all the way up to the edge of the magnetic dome in compositional space.[15] While it can be difficult to non-arbitrarily compare compositions between studies, the T_N can be used as a metric for determining whether a sample has higher or lower composition than another. The 3 samples exhibiting the C_4 phase from dilatometry each have a lower T_N than the 3 samples reported here (64.5, 54.5, and 45.5 K; and 94.0, 86.7, and 74.8 K, respectively). This means that the compositions of those samples are all higher than the compositions of the samples reported here. According to dilatometry the C_4 phase fraction is very large, possibly even 100%. This differs from our result, where only a small phase fraction is observed at a lower composition than in dilatometry, which either partially or entirely goes away at higher compositions.

The question remains on how to explain the discrepancy. A simple, yet unlikely, explanation would be that the $x = 0.24$ sample reported here has a large distribution of local stoichiometries that overlap with the regime reported via dilatometry. However, this does not comport with observation, since this would mean that the structural transition at T_N would be extremely broad, with at least 10% of the sample remaining tetragonal below 65 K. This nominal $x = 0.24$ sample (average estimated composition $x = 0.237$) shows no tetragonal phase below 80 K in the x-ray data, which means that more than 99% of the sample has a composition less than 0.249 (the average composition of the $x = 0.25$ sample, which has a $T_N = 74.8K$) let alone the higher relative compositions reported in dilatometry ($T_{N,max} = 64.5$ K).[15] This means that the small phase fraction is intrinsic to this composition window, and not from an overlap with a nearby, larger dome.

Another explanation could be that the application of uniaxial stress necessary to measure dilatometry may change the properties enough to shift phase boundary lines (see Hassinger *et al.*[16]). Yet another alternative is that the existence of the C_4 phase may be sensitive to preparation method, such that an uncontrolled parameter may have a strong effect on its formation. For example, in the related β-FeSe system, the presence of trace amounts of oxygen has a strong effect on the superconducting properties.[17]

IV. CONCLUSION

The combined neutron and x-ray powder diffraction on $Ba_{0.76}K_{0.24}Fe_2As_2$ shows evidence of a second, minority phase below 30 K. The structural and magnetic features of the secondary phase provide direct evidence that it is the same electronic phase as the previously reported tetragonal magnetic phase in $Ba_{1-x}Na_xFe_2As_2$,[4] but with a reduced stability, possibly due to the larger cation size. This provides evidence that the C_4 phase is a universal feature of the hole-doped 122 family of iron-based superconductors. The resulting phase diagram is similar to the one recently reported by Böhmer *et al*[15], although they claim that the tetragonal phase fraction is 100%. The fact that we observe it as a minority phase suggests that the stability of the C_4 phase is extremely sensitive to subtle changes in sample composition and measurement conditions. We have proposed that the C_4 phase is evidence for itinerant spin-nematic theory, in which the coupled magnetic and structural transitions are due to magnetic fluctuations caused by Fermi surface nesting. This theory predicts that the C_2 and C_4 phases have very similar free energies close to the suppression of C_2 order,[4] which is consistent with the delicate stability of the C_4 phase. In this model, the C_4 SDW results from a simultaneous coupling between Fermi surfaces along two in-plane directions, rather than just one in the C_2 phase, providing a natural explanation for the stronger phase competition with superconductivity evident in the phase diagram.

ACKNOWLEDGMENTS

This work was supported by the U.S. Department of Energy, Office of Science, Materials Sciences and Engineering. This research used resources of the Advanced Photon Source, a U.S. Department of Energy (DOE) Office of Science User Facility operated for the DOE Office of Science by Argonne National Laboratory under Contract No. DE-AC02-06CH11357, and was aided by the 11-BM beam scientist M. Suchomel. Experiments at the

ISIS Pulsed Neutron and Muon Source were supported by a beam time allocation from the Science and Technology Facilities Council.

* jallred@anl.gov

[1] H. Kontani, Y. Inoue, T. Saito, Y. Yamakawa, and S. Onari, Solid State Communications Special Issue on Iron-based Superconductors, **152**, 718 (2012).

[2] R. M. Fernandes, A. V. Chubukov, and J. Schmalian, Nature Physics **10**, 97 (2014).

[3] P. Dai, J. Hu, and E. Dagotto, Nature Physics **8**, 709 (2012).

[4] S. Avci, O. Chmaissem, J. M. Allred, S. Rosenkranz, I. Eremin, A. V. Chubukov, D. E. Bugaris, D. Y. Chung, M. G. Kanatzidis, J.-P. Castellan, J. A. Schlueter, H. Claus, D. D. Khalyavin, P. Manuel, A. Daoud-Aladine, and R. Osborn, Nature Communications **5**, 3845 (2014).

[5] S. Avci, J. M. Allred, O. Chmaissem, D. Y. Chung, S. Rosenkranz, J. A. Schlueter, H. Claus, A. Daoud-Aladine, D. D. Khalyavin, P. Manuel, A. Llobet, M. R. Suchomel, M. G. Kanatzidis, and R. Osborn, Physical Review B (Condensed Matter and Materials Physics) **88**, 094510 (2013).

[6] S. Avci, O. Chmaissem, E. A. Goremychkin, S. Rosenkranz, J.-P. Castellan, D. Y. Chung, l. S. Todorov, J. A. Schlueter, H. Claus, M. G. Kanatzidis, A. Daoud-Aladine, D. D. Khalyavin, and R. Osborn, Physical Review B (Condensed Matter and Materials Physics) **83**, 172503 (2011).

[7] F. Wasser, A. Schneidewind, Y. Sidis, S. Wurmehl, S. Aswartham, B. Buchner, and M. Braden, Physical Review B) **91**, 060505 (2015).

[8] D. D. Khalyavin, S. W. Lovesey, P. Manuel, F. Krüger, S. Rosenkranz, J. M. Allred, O. Chmaissem, and R. Osborn, Physical Review B **90**, 174511 (2014).

[9] S. Nandi, M. G. Kim, A. Kreyssig, R. M. Fernandes, D. K. Pratt, A. Thaler, N. Ni, S. L. Bud'ko, P. C. Canfield, J. Schmalian, R. J. McQueeney, and A. I. Goldman, Physical Review Letters **104**, 057006 (2010).

[10] M. Rotter, M. Pangerl, M. Tegel, and D. Johrendt, Angewandte Chemie International Edition **47**, 7949 (2008).

[11] S. Avci, O. Chmaissem, D. Y. Chung, S. Rosenkranz, E. A. Goremychkin, J.-P. Castellan, l. S. Todorov, J. A. Schlueter, H. Claus, A. Daoud-Aladine, D. D. Khalyavin, M. G. Kanatzidis, and R. Osborn, Physical Review B (Condensed Matter and Materials Physics) **85**, 184507 (2012).

[12] A. C. Larson and R. B. Von Dreele, Los Alamos National Laboratory Report **86-748** (2000).

[13] B. H. Toby, J. Appl. Cryst. **34**, 210 (2001).

[14] J. M. Allred, K. M. Taddei, D. E. Bugaris, S. Avci, D. Y. Chung, H. Claus, C. dela Cruz, M. G. Kanatzidis, S. Rosenkranz, R. Osborn, and O. Chmaissem, Phys. Rev. B **90**, 104513 (2014).

[15] A. E. Böhmer, F. Hardy, L. Wang, T. Wolf, P. Schweiss, and C. Meingast, ArXiv e-prints (2014), arXiv:1412.7038 [cond-mat.supr-con].

[16] E. Hassinger, G. Gredat, F. Valade, S. R. de Cotret, A. Juneau-Fecteau, J.-P. Reid, H. Kim, M. A. Tanatar, R. Prozorov, B. Shen, H. H. Wen, N. Doiron-Leyraud, and L. Taillefer, Physical Review B (Condensed Matter and Materials Physics) **86**, 140502 (2012).

[17] T. M. McQueen, Q. Huang, V. Ksenofontov, C. Felser, Q. Xu, H. Zandbergen, Y. S. Hor, J. Allred, A. J. Williams, D. Qu, J. Checkelsky, N. P. Ong, and R. J. Cava, Phys. Rev. B **79**, 014522 (2009).